Eur. Phys. J. A **25**, s01, 245–250 (2005)
DOI: 10.1140/epjad/i2005-06-171-4

EPJ A direct
electronic only

First experiments on transfer with radioactive beams using the TIARA array

W.N. Catford[1,a], R.C. Lemmon[2], M. Labiche[3], C.N. Timis[1], N.A. Orr[4], L. Caballero[5], R. Chapman[3], M. Chartier[6], M. Rejmund[7], H. Savajols[7], and the TIARA Collaboration

[1] Department of Physics, University of Surrey, Guildford, Surrey GU2 7XH, UK
[2] Nuclear Structure Group, CCLRC Daresbury Laboratory, Daresbury, Warrington WA4 4AD, UK
[3] University of Paisley, Paisley, Scotland PA1 2BE, UK
[4] Laboratoire de Physique Corpusculaire, IN2P3-CNRS, ISMRA and Université de Caen, F-14050 Caen, France
[5] Instituto de Fisica Corpuscular, CSIC-Universidad de Valencia, E-46071 Valencia, Spain
[6] Department of Physics, The University of Liverpool, Liverpool L69 7ZE, UK
[7] GANIL, BP 55027, 14076 Caen Cedex 5, France

Received: 22 October 2004 /
Published online: 11 August 2005 –

Abstract. Results from a study in inverse kinematics of the ^{24}Ne(d, pγ)^{25}Ne reaction, using a radioactive beam of ^{24}Ne from the SPIRAL facility at GANIL, are reported. First, a brief overview is given of several methods using radioactive beams to study the classic single-nucleon transfer reactions such as (d, p) or (d, t)/(d, ^{3}He), where the experimental design is strongly influenced by the extreme inverse kinematics. A promising approach to deliver good energy resolution is to combine a high geometrical efficiency for kinematically complete charged particle detection with a high efficiency array for gamma-ray detection. One of the first dedicated set-ups for this type of experiment is the TIARA silicon strip array combined with the EXOGAM segmented germanium array. Together they comprise a highly compact, position-sensitive particle array with 90% of 4π coverage, mounted inside a cubic arrangement of four segmented gamma-ray detectors in very close geometry with 67% of 4π active coverage. Using this setup, the structure of ^{25}Ne has been studied via the (d, p) reaction. A pure ISOL beam of 10^5 s^{-1} of ^{24}Ne at 10 MeV/A was provided by SPIRAL and bombarded a CD_2 target of 1 mg/cm^2. The ^{25}Ne was detected at the focal plane of the VAMOS spectrometer where the direct beam was separated and intercepted. Reaction protons were detected in coincidence with little background. Four resolved peaks were recorded between $E_x = 0$ and 4 MeV. The data confirm and extend the results from a multinucleon transfer study using the (^{13}C,^{14}O) reaction. Further information has been obtained using the energies of coincident gamma-rays. The reactions ^{24}Ne(d, dγ)^{24}Ne, ^{24}Ne(d, t)^{23}Ne and ^{24}Ne(d, ^{3}He)^{23}F were recorded simultaneously and analysis of these is also underway.

PACS. 25.60.-t Reactions induced by unstable nuclei – 25.60.Je Transfer reactions – 27.30.+t Properties of specific nuclei listed by mass ranges: $20 \leq A \leq 38$

1 Introduction

Nucleon transfer reactions provide a valuable means to identify and study nuclear levels, and in particular to identify the levels that have a simple single-particle structure close to closed shells. Experiments using single-nucleon transfer become technically feasible with intensities of typically > 1000 or $> 10^4$ pps, depending on the experimental approach. The present work concentrates on light-ion–induced transfer, and in particular reactions such as (d, p) and (d, t) or (p, d) induced by hydrogen isotopes. The experiments are performed in inverse kinematics with a radioactive beam incident on hydrogen target nuclei. A major aim is to measure the angular distribution characterizing the transferred angular momentum, and this results in choosing to measure the light particles that come from the target. This, in turn, places a limit on the target thickness that is compatible with the desired energy resolution (of order 0.5 MeV). As discussed below, these various criteria have led to an approach using triple coincidences between the two charged products of the binary reaction, plus any de-excitation gamma-ray emitted by the heavy product.

[a] Conference presenter; e-mail: W.Catford@surrey.ac.uk

2 The experimental perspective

The experimental design is determined largely by the properties of the extreme inverse kinematics [1,2]. A characteristic feature is that the light particles from reactions such as (d, t) or (p, d) —in which the radioactive beam loses a nucleon— are focussed to come within a cone of angles forward of typically 40°. In contrast, protons from (d, p) emerge at backward angles and typically require to be detected between 90° and 180° in the laboratory frame. The energies have a relatively minor dependence on the mass and velocity of the projectile, and thus a dedicated array with general utility can be envisioned.

It can be remarked that there is some dependence that remains, on the beam velocity, which does have some experimental implications for detecting the light particles. Whilst the overall form of the velocity vector diagrams [2] is essentially independent of the beam mass or velocity, the size of the diagram scales with these quantities. With the notation of ref. [2], the velocities $v_{\rm e}$ and $v_{\rm cm}$ have lengths $\sqrt{M_R/M_{\rm e}}$ and $1/\sqrt{M_P/(q \times M_T)}$, respectively (where q is between 1.0 and 1.5 in most cases and the labels R, e, P and T refer to the heavy recoil, light ejectile, projectile and target). Since $M_P \approx M_R$ (because only one nucleon is transferred, and the projectile is assumed to have a large mass compared to the target) then the lengths of $v_{\rm e}$ and $v_{\rm cm}$ both scale as $\sqrt{M_P}$ to a first approximation. Also, the unit of length for the velocity vectors in this analysis is given [3] by $\sqrt{2qE_{\rm cm}/(M_R + M_{\rm e})}$ which is approximately proportional to $\sqrt{(E/A)_{\rm beam}/M_P}$ assuming again that $M_P \approx M_R$ and that each of these masses is large compared to the light-particle masses. Combining these two length factors, the overall scaling of the vector diagram varies approximately as $\sqrt{(E/A)_{\rm beam}}$ and hence the kinetic energies of backward or forward going light particles, or indeed the rate of energy increase with angle for elastically scattered particles near 90°, are roughly proportional to $(E/A)_{\rm beam}$.

One of the earliest experiments of the type discussed here was a study of the (d, p) reaction on a ^{56}Ni projectile, for astrophysical interest [4]. The experimental set-up included a silicon array that covered the backward angular range that is important for (d, p) in inverse kinematics. The data from that experiment highlight the challenges faced by this type of work, in terms of limited statistics and resolution, but also they serve to demonstrate how a useful angular distribution can be obtained with only a limited number of counts.

An alternative approach was used in a study of (p, d) induced by a ^{11}Be beam [5]. In this case, the angular information was obtained from the beam-like particle ^{10}Be as measured in a magnetic spectrometer. It was essential to tag reactions induced by the hydrogen rather than the carbon in the (CH_2) target, using light-ion coincidences. A pure cryogenic target can avoid that problem but the coincidence is still required to avoid any ambiguity over the transfer reaction mechanism. In any case, a general feature of the kinematics is that the angular resolution required in the measurement of the beam-like particle becomes too demanding for beams that are somewhat heavier than beryllium. For this reason and others [6], in search of a more general technique, the method using triple coincidences (with gamma-rays) was selected for the present experiment and its related programme.

A method that relies on triple coincidences places very demanding requirements on the efficiencies of each detection system. The TIARA array was constructed so as to achieve the maximum possible gamma-ray detection efficiency with the available detectors. Germanium clover detectors with additional electronic segmentation were chosen, where the segmentation was required so as to minimise the Doppler broadening introduced by the emitting nuclei, which have velocities essentially equal to that of the incident beam. At the same time, the idea was to have the capability of using quite intense radioactive beams up to 10^8–10^9 pps, in which case gamma-ray detectors would need to be shielded from scattered beam, which can give subsequent gamma-rays from radioactive decay. These conflicting goals were achieved by using a very close geometry for the gamma-ray detectors and an open-ended barrel around the target for the charged particles. In turn, this placed strong limitations on the size and hence complexity of the charged particle detection system, and in the first version of TIARA there is no ΔE-E particle identification for the light particles, so reliance is placed instead on identifying the beam-like particles.

Other recent light-ion–induced single-nucleon transfer studies, performed in inverse kinematics with radioactive beams, are reported at this conference. For example, several (d, p) studies using a similar technique but without gamma-ray detection are reported using beams of ^{82}Ge and ^{84}Se [7] and also ^{124}Sn [8]. A study of (α, t) with a beam of ^{22}O is also reported, using the method of measuring just the beam-like particle [9].

3 Experimental details

The first radioactive beam experiment using the TIARA array was performed at GANIL using a pure ^{24}Ne beam of 1×10^5 pps, provided by the SPIRAL facility. The beam was limited in emittance to 8π mm.mrad so as to restrict the size of the beam spot on target to approximately 1.5–2.0 mm diameter. No beam tracking was employed. The energy was 10.6 MeV/A. The target was deuterated polythene $(CD_2)_n$ with a thickness of 1.0 mg/cm^2 and this thickness was the limiting factor in the excitation energy resolution that was achieved using just the charged particles. A summary of the experimental setup is shown in fig. 1.

The TIARA array [10] in its present configuration [11] has the active area of silicon strip detectors spanning 85% of 4π. The detectors have intrinsic thicknesses (without allowing for angle of incidence) of 400–500 μm. The main feature is an octagonal shaped barrel made from 8 silicon detectors, each approximately 100 mm in length and comprising 4 resistive strips, position sensitive along the beam direction. This barrel by itself spans approximately 80% of 4π, from 35° to 145°. Further, it has a radius of

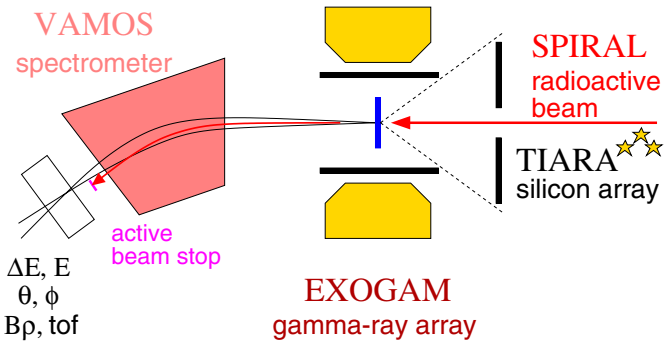

Fig. 1. Schematic experimental set-up. The silicon barrel and annular arrays recorded light charged particles; beam-like particles were physically separated from the beam using VAMOS [12] at zero degrees, and EXOGAM [13,14] surrounded the target to detect gamma-rays.

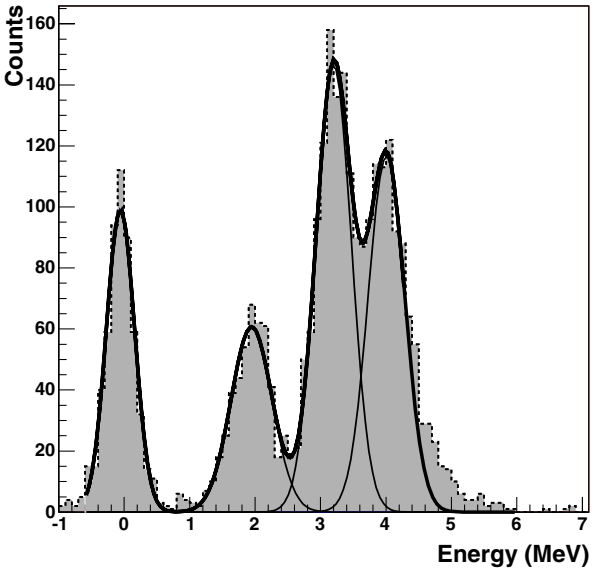

Fig. 2. Excitation energy spectrum for ^{25}Ne reconstructed from proton energies and angles for (d, p) data recorded with a radioactive beam of ^{24}Ne.

only 35 mm and there is a reduced radius for the vacuum chamber in the region of the barrel so that gamma-ray detectors can be placed as close as 50 mm from the target to maximize their efficiency.

Beam and reaction particles coming forward of 4° relative to the beam escaped the most forward part of TIARA and entered into the VAMOS spectrometer [12] which was operated in momentum-dispersive mode. The direct beam was intercepted with an active scintillator finger mounted in front of the standard focal plane detector system. The kinematics were such that the finger did not intercept any of the ^{25}Ne products from (d, p) reactions for which the proton emerged at a laboratory angle of 100° or greater. Reaction products from the reactions (d, t) and (d, ^{3}He), leading to ^{23}Ne and ^{23}F respectively, were on the focal plane and well clear of the finger. At the focal plane, the angle and position were measured in two dimensions, and the energy loss, total energy and time of flight were also measured for each ion.

Gamma-rays were recorded using four detectors from the EXOGAM array [13,14] mounted so that their square front faces almost touched, forming four sides of a cube. This put the front faces at 50 mm from the target. For the ^{24}Ne experiment, the segmentation information from the detectors was not available and only the central contact energy signal in each clover leaf was recorded. Segmentation would reduce the energy resolution, which is limited by Doppler broadening, by a factor of two. In the present work, this resolution was 50 keV (fwhm) at 1 MeV. The full energy peak efficiency in this configuration is approximately 17% at 1.332 MeV, but the effective efficiency was 1 or 2 percent in the present experiment due to an intermittent discriminator fault.

The whole of the TIARA and EXOGAM array response has been modelled in a simulation using GEANT4 [15], including a verification of the algorithm employed for add-back of EXOGAM signals in the very close TIARA geometry. Here, "add-back" refers to the summing in software analysis of the two energy signals obtained when two leaves of a clover are triggered in the same event, and also the assignment of the primary interaction for Doppler calculations. Such events comprised approximately 20% of the data.

4 Results

When a two-dimensional plot is made of particle energies (recorded in TIARA) as a function of scattering angle, gated on the requirement that a beam-like particle reaches the focal plane, it is found to be free of any significant background —especially backward of 90°. Such a plot (omitted due to space) highlights the loci in the backward hemisphere corresponding to different states populated in (d, p). The overall spectrum is dominated by the elastic scattering of deuterons from the target. This produces a kinematic line that rises in energy rapidly with decreasing angle, just forward of 90°. The kinematic loci from (d, t) reactions are discernible in the forward annular detectors and in the forward part of the barrel. The data for each of these other channels will require proper particle identification using the VAMOS focal plane parameters to identify the beam-like particles. This work is still in progress. The analysis reported here requires simply that there is a particle at the focal plane, in coincidence with TIARA. The angular range of interest for the (d, p) reaction, backward of 100° in the laboratory frame, corresponds simultaneously to the angles for which the proton is completely stopped by the barrel detector and the coincident particle at the focal plane avoids the active beam stopper.

From the calibrated energy and angle of the detected particles in TIARA, the excitation energy of the corresponding ^{25}Ne nucleus can be calculated. Figure 2 shows the spectrum corresponding to events recorded in the annular array at backward angles, behind the barrel. The resolution in excitation energy is 500 keV (fwhm). The

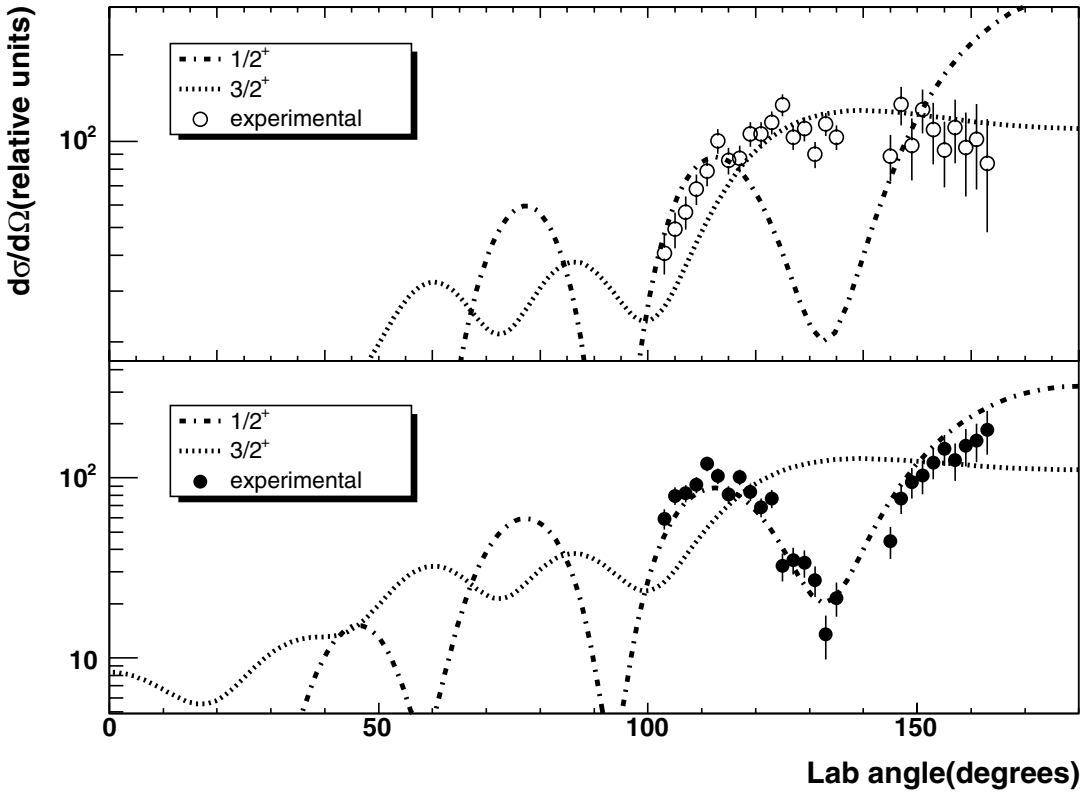

Fig. 3. Proton angular distributions measured for groups from (d, p) populating states in ^{25}Ne: lower panel for the ground-state peak, upper panel for the peak at 2 MeV. Preliminary reaction calculations for transferred angular momentum of 0 (darker, dot-dashed line) and 2 units (dotted line) are shown.

data from the barrel are consistent in terms of the peak centroid positions, but show a poorer average resolution of 1100 keV. An analysis of the contributions to the resolution using the approach of ref. [6] is consistent with these results and reveals that two angle-dependent terms become important and dominate the resolution in the barrel region. These terms arise firstly from the kinematics, whereby the calculated excitation energy is more critically dependent on the angle in the region closer to 90°, and secondly from the effects of multiple angular scattering which is accentuated when the particle exits from the target through more material, at a shallow angle to the surface.

Proton angular distributions $\mathrm{d}\sigma/\mathrm{d}\Omega$ were extracted for the d(^{24}Ne, p)^{25}Ne reaction by selecting events in the ground-state peak and in the peak shown at an excitation energy of 2 MeV in fig. 2. Figure 3 shows these angular distributions, together with preliminary reaction calculations employing global optical potential parameters and the Johnson-Soper prescription [16] to account for deuteron breakup to the continuum.

The transferred angular momentum for the ground state is assigned as $\ell = 0$, which implies a spin and parity of $1/2^+$. For the group at 2 MeV, the angular distribution is clearly different. It shows quite good agreement with the calculation for $\ell = 2$ and this implies a state or states with spin and parity $(3/2,\ 5/2)^+$. Angular distributions for the incompletely resolved peaks at 3.3 and 4.0 MeV are still under analysis.

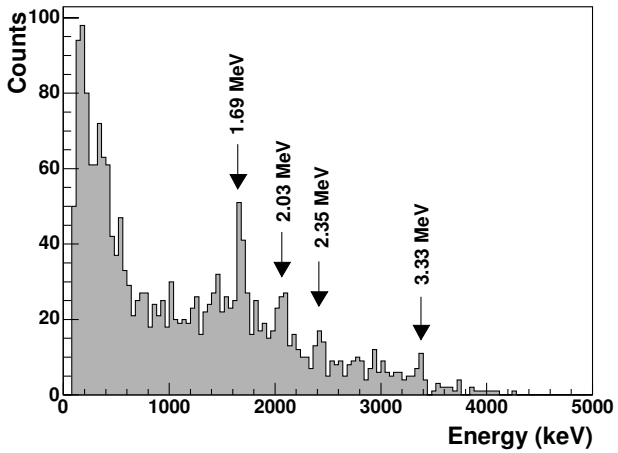

Fig. 4. Gamma-ray energy spectrum recorded in coincidence with all protons from the reaction d(^{24}Ne, p)^{25}Ne. A Doppler shift correction has been applied to the gamma-ray energies.

The events in fig. 2 corresponding to the peak spanning the ground-state region are all removed from the spectrum when a coincidence with gamma-rays is required. Thus, the peak corresponds simply to population of the ground state.

The remainder of the peaks in fig. 2 are in coincidence with gamma-rays. Figure 4 shows the summed spectrum

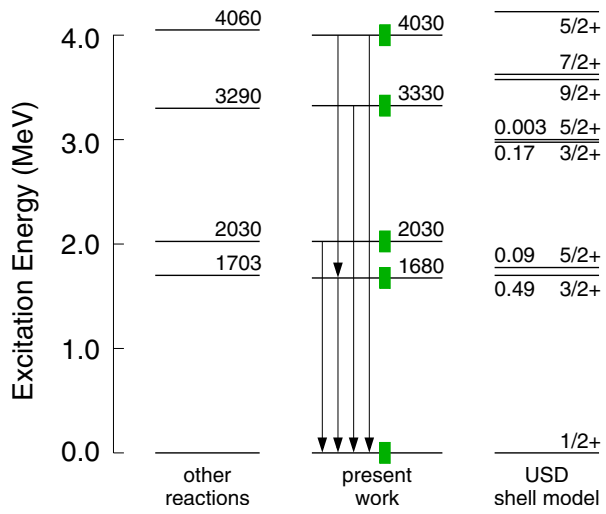

Fig. 5. Energy levels in ^{25}Ne and their excitation energies in keV. The column "other reactions" refers to previous work (see text). Shell model results are labelled with spin and parity and are from ref. [17] with selected spectroscopic factors as calculated in ref. [18]. The present results show the observed gamma-ray transitions and an indication of the effective fwhm resolution in energy.

of these gamma-rays for all of the states between 2 and 5 MeV in ^{25}Ne. The gamma-ray energy for each event has been corrected for the Doppler shift imparted by the ^{25}Ne, which always has a velocity of magnitude approximately $0.15c$ and is always aligned within two degrees of the beam direction. The precise value of $\langle \beta \cos\theta_\gamma \rangle$ required for the Doppler correction can be inferred from the data by comparing spectra from the elements of the clover situated forward and backward of the target position. In addition, an add-back procedure has been applied, as discussed in sect. 3. The energy resolution was measured to be 100 keV (fwhm) at 1.9 MeV using data from the d(^{24}Ne, d′)^{24}Ne* reaction. This is consistent with the limitation imposed by Doppler broadening due to the finite size of each Ge detector crystal.

The gamma-ray energy spectrum is displayed in fig. 4 and shows several clear peaks. The origin of the general increase in counts below 0.5 MeV is still being investigated. At higher energies, the spectrum abruptly drops to zero above about 4 MeV. A maximum gamma-ray energy of 4.03 MeV is inferred, which is consistent with the excitation energy of the highest particle group observed.

Exclusive gamma-ray energy spectra have been extracted for each of the three excited state peaks seen in fig. 2, and show clear differences despite the limited statistics. In particular, the gamma-ray at 1.69 MeV is only clearly evident in association with the 4.03 MeV peak in the particle spectrum. Any direct population of a 1.68 MeV state in ^{25}Ne must be quite weak relative to the 2.03 MeV state.

The gamma-ray decay scheme inferred from the data is included in fig. 5.

5 Discussion

The energy levels observed in the present work are displayed in fig. 5, along with previous information from the literature and the predictions for positive parity states according to the shell model within a full *sd*-shell basis [17]. The shell model levels are not explicitly labelled in energy, but rather the spin and parity are given, along with the single neutron spectroscopic factors for selected levels as calculated in ref. [18].

The previous data come from two heavy ion transfer studies and also a study of β-delayed gamma-rays in ^{25}Ne following the decay of ^{25}F [19]. The two heavy ion reaction studies each involved the removal of two protons from ^{26}Mg and the addition of a neutron. The selectivity of the (^{7}Li,^{8}B) reaction [20] and the (^{13}C,^{14}O) reaction [18] are slightly different, probably due to the cluster structure of ^{7}Li. Some further considerations are mentioned in ref. [18] and in the discussion below. The β-decay data give one rather clear result, namely a more precise energy than the transfer experiments for the state at 1.703 MeV.

The present data indicate that the level at 2.03 MeV is populated much more strongly in the (d, p) reaction than the level seen at 1.68 MeV, and hence that the $\ell = 2$ assignment from fig. 3 rightly refers to the 2.03 MeV level. It seems likely that the level measured to be at 1.68 MeV can be associated with the level measured more precisely to be at 1.703 MeV in the β-decay work. It is not entirely clear from the gamma-ray spectrum to what extent the 1.68 MeV level is populated directly, or whether it is populated at all; this uncertainty is due to counts in the compton edge of the 2.03 MeV gamma-ray. However, it is clear that the relative strengths between the levels at 1.68 MeV and 2.03 MeV in (d, p) is exactly opposite to that observed using the (^{13}C,^{14}O) reaction. Insofar as both reactions involve the addition of a neutron to an $N = 14$ nucleus, this is perhaps surprising, but the reaction mechanism is much more complex in the case of (^{13}C,^{14}O). Woods [18] used the larger spectroscopic factor of the $J^\pi = 3/2^+$ state to argue that the peak observed at 1.7 MeV in (^{13}C,^{14}O) corresponded to this state. By the same criteria, it could be argued from the (d, p) result that the 2.03 MeV state is in fact the $3/2^+$. Further study of this question is underway. It may be remarked that the population of the $5/2^+$ state in (^{13}C,^{14}O) can proceed by the transfer of a neutron to the vacant $s_{1/2}$ orbital, accompanied by the removal of an $\ell = 2$ di-proton cluster from the ^{26}Mg target. The neutron step is the same as the transfer that produces the ground state strongly. It is a general feature of such reactions (see, for example, the discussion in ref. [21]) that higher ℓ transitions are favoured by the reaction dynamics and this would enhance the $\ell = 2$ pathway relative to its amplitude according to simple structure considerations. This provides at least the possibility that the (^{13}C,^{14}O) reaction may actually favour the $5/2^+$ state over the $3/2^+$ state.

Additional information about which states are likely to be populated in ^{25}Ne by the (d, p) reaction can be inferred from the results [22] of a (d, p) study performed using a target of ^{26}Mg, an isotone of ^{24}Ne. That study indicated in particular that significant strength is to be expected for

the population of negative parity states in the region of 3 to 4 MeV. Thus, it seems likely that the levels seen here at 3.33 MeV and 4.03 MeV in ^{25}Ne represent transfer to the $0f_{7/2}$ and $1p_{3/2}$ orbitals.

In summary, the present data indicate clearly that the ground state in ^{25}Ne is populated by $\ell = 0$ transfer in the (d, p) reaction, and hence that it has spin and parity $1/2^+$ which is consistent with the prediction of the simple shell model and also a full USD calculation [17]. The state seen at 2.03 MeV has a distribution that is well described by a transfer of two units of angular momentum. This is consistent with both of the states predicted near 1.7 MeV in the USD calculation. Further interpretation of these results and further analysis of the results for the two levels observed above 3 MeV (likely to be negative parity levels) is expected to give interesting information about the changing shell structure for neutrons in the $N = 14$ to $N = 16$ region. This is currently a topic of great research interest [23,24,25]. The results of this first experiment using the TIARA array are also very encouraging in terms of what they demonstrate should be possible with transfer reaction studies in the future.

References

1. W.N. Catford, Acta Phys. Pol. B **32**, 1049 (2001).
2. W.N. Catford, Nucl. Phys. A **701**, 1 (2002).
3. W.N. Catford *et al.*, Nucl. Instrum. Methods A **247**, 367 (1986).
4. K.E. Rehm *et al.*, Phys. Rev. Lett. **80**, 676 (1998).
5. J.S. Winfield *et al.*, Nucl. Phys. A **683**, 48 (2001).
6. J.S. Winfield, W.N. Catford, N.A. Orr, Nucl. Instrum. Methods A **396**, 147 (1997).
7. J.S. Thomas *et al.*, these proceedings.
8. K.L. Jones *et al.*, these proceedings.
9. S. Michimasa *et al.*, these proceedings.
10. W.N. Catford, C.N. Timis, M. Labiche, R.C. Lemmon, G. Moores, R. Chapman, in *CAARI 2002*, edited by J.L. Duggan, I.L. Morgan, AIP Conf. Proc. **680**, 329 (2003).
11. W.N. Catford, R.C. Lemmon, C.N. Timis, M. Labiche, L. Caballero, R. Chapman, in *Tours Symposium V*, edited by M. Arnould *et al.*, AIP Conf. Proc. **704**, 185 (2004).
12. H. Savajols *et al.*, Nucl. Instrum. Methods B **204**, 146 (2003).
13. W.N. Catford, J. Phys. G **24**, 1377 (1998).
14. J. Simpson *et al.*, Acta Phys. Hung. A: Heavy Ion Phys. **11**, 159 (2000).
15. S. Agostinelli *et al.*, Nucl. Instrum. Methods A **506**, 250 (2003).
16. R.C. Johnson, P.J.R. Soper, Phys. Rev. C **1**, 976 (1970).
17. B.A. Brown, on-line database "*sd*-shell USD energies", `http://www.nscl.msu.edu/~brown/resources/SDE.HTM`.
18. C.L. Woods *et al.*, Nucl. Phys. A **437**, 454 (1985).
19. A.T. Reed *et al.*, Phys. Rev. C **60**, 024311 (1999).
20. K.H. Wilcox *et al.*, Phys. Rev. Lett. **30**, 866 (1973).
21. W.N. Catford *et al.*, Nucl. Phys. A **503**, 263 (1989).
22. F. Meurders, A. Van Der Steld, Nucl. Phys. A **230**, 317 (1974).
23. A. Ozawa *et al.*, Phys. Rev. Lett. **84**, 5493 (2000).
24. T. Otsuka *et al.*, Phys. Rev. Lett. **87**, 082502 (2001).
25. M. Stanoiu *et al.*, Phys. Rev. C **69**, 034312 (2004).